Received: 28 April 2024 | Revised: 14 July 2024 | Accepted: 27 July 2024
DOI: 10.1002/ca.24208

COMMUNICATION

CLINICAL ANATOMY WILEY

Optimizing the selection of the endoscopically assisted supracerebellar transtentorial approach to the medial temporo-occipital region: Clinical application of one novel grid coordinate system

Bon-Jour Lin[1,2] | Da-Tong Ju[1] | Chin Lin[3,4,5] | Dueng-Yuan Hueng[1] | Yuan-Hao Chen[1] | Hsin-I Ma[1] | Ming-Ying Liu[1]

[1]Department of Neurological Surgery, Tri-Service General Hospital, National Defense Medical Center, Taipei, Taiwan, ROC

[2]Graduate Institute of Medical Sciences, National Defense Medical Center, Taipei, Taiwan, ROC

[3]Medical Technology Education Center, School of Medicine, National Defense Medical Center, Taipei, Taiwan, ROC

[4]School of Public Health, National Defense Medical Center, Taipei, Taiwan, ROC

[5]Artificial Intelligence of Things Center, Tri-Service General Hospital, National Defense Medical Center, Taipei, Taiwan, ROC

Correspondence
Bon-Jour Lin, Department of Neurological Surgery, Tri-Service General Hospital, No. 325, Section 2, Cheng-Kung Road, Neihu 114 Taipei, Taiwan, ROC.
Email: coleman0719@gmail.com

Funding information
Tri-Service General Hospital of Taiwan's Medical Research Project (TSGH-D-111088 and TSGH-D-112095)

Abstract

The endoscopically assisted supracerebellar transtentorial (eSCTT) approach is advocated for managing pathologies of the medial temporo-occipital region, but quantitative analysis is currently lacking. The aims of this study were to establish a grid coordinate system on the tentorium to model the anatomical relationship between medial temporo-occipital region pathology and the slope of the tentorium, and then to compare the paramedian eSCTT and extreme-lateral eSCTT approaches quantitatively. Bilateral paramedian and extreme-lateral eSCTT approaches were used to dissect three adult cadaveric heads anatomically. A grid coordinate system was established on the tentorium, and the angles of attack and depth of the surgical corridor of each coordinate point were obtained so that the two eSCTT approaches could be compared statistically. The measurements were then analyzed to determine the condition for selecting each eSCTT approach, and its clinical feasibility was assessed in three patients with large tumors in the medial temporo-occipital region. For coordinate points where the *X*-coordinate on the grid coordinate system was 1 cm outside the apex of the tentorium, the paramedian eSCTT approach had a significantly wider angle of attack and shorter depth of surgical corridor than the extreme-lateral eSCTT approach. In contrast, the extreme-lateral eSCTT approach was better for coordinate points where the *Y*-coordinate on the grid coordinate system was 1 cm in front of the apex of the tentorium. The long axis of each patient's tumor was projected on to the tentorium and its corresponding coordinate points were used to match the more appropriate eSCTT approach. Preliminary results for three patients treated with the eSCTT approach for large tumors in the medial temporo-occipital region were encouraging. When the eSCTT approach is applied to manage a large tumor of the medial temporo-occipital region, assessment of the long axis of the tumor and knowledge of the selective condition for each eSCTT approach can help in clinical decision-making.

KEYWORDS
endoscopic, supracerebellar infratentorial, supracerebellar transtentorial, temporo-occipital

1 | INTRODUCTION

Clinical application of the supracerebellar transtentorial (SCTT) approach to managing supratentorial lesions was first reported by Voigt and Yasargil (1976) in a case of parahippocampal cavernous angioma. Thanks to a more detailed understanding of neuroanatomy and the low morbidity of the procedure, the SCTT approach is being increasingly used for supratentorial pathologies of the medial temporal region, thalamus, and lateral ventricle (Campero et al., 2006; de Oliveira et al., 2010; Marcus et al., 2013; Türe et al., 2012; Weil et al., 2015). However, uncomfortable ergonomics and a restricted operative view are major disadvantages of the microsurgical SCTT approach to treating supratentorial lesions, especially when the lesion is large.

In the literature on the treatment of supratentorial lesions via this approach, most cases have involved relatively small tumors, and to date there has been no quantitative analysis of this approach to selected larger tumor masses. For large tumors, not only the tumor itself but also its anatomical relationship with the slope of the tentorium must be considered in preoperative planning. Moreover, it is important to know whether the choice of location for suboccipital craniotomy, and for the supracerebellar infratentorial (SCIT) approach, affects the operative result (Cavalcanti et al., 2019; Matsuo et al., 2017). The endoscopically-assisted SCTT (eSCTT) approach has recently been described as having an even more favorable outcome. Endoscopy appears to overcome the limitations of the microscopic SCTT approach effectively by providing better visualization and facilitating deeper access (Coca et al., 2022; Marcus et al., 2013; Villanueva et al., 2015).

In this study, we first built a grid coordinate system on the tentorium to mimic the anatomical relationship between the temporo-occipital lesion and the slope of the tentorium. We then compared the paramedian and extreme-lateral eSCTT approaches quantitatively. The purpose of the study was analyze different eSCTT approaches for treating large temporo-occipital lesions.

2 | MATERIALS AND METHODS

This study was conducted after Institutional Review Board approval was obtained (IRB: B202005127). Three formaldehyde-fixed, silicone-injected cadaveric heads were dissected in the Skull Base Laboratory of the National Defense Medical Center. Pre-procedure thin-slice computed tomography coupled with the StealthStation® S7® Navigation System (Medtronic, Minneapolis, MN, USA) was used to collect and analyze data for each cadaveric head.

2.1 | Surgical dissections

Each cadaveric head was fixed in a Mayfield head holder to simulate a sitting position, and the upper surface of the tentorium was exposed after the paired occipital lobes were removed (Figure 1A). The boundaries of exposure were the superior petrosal sinuses anteriorly, the tentorial incisura medially, and the transverse sinuses posterolaterally. The lower surface of the tentorium was then exposed through the paramedian and extreme-lateral eSCTT approaches executed on each side of the cadaveric head. A total of six paramedian and six extreme-lateral eSCTT approaches were established in the three cadaveric heads.

2.2 | Paramedian eSCTT approach

A 3-cm-wide rectangular suboccipital craniotomy was performed by making a single vertical incision equidistant from the external auditory canal and the midline; the transverse sinus constituted the upper margin of the bone flap (Figure 2A). The dura was cut along the edge of the bone flap and deflected upward along the transverse sinus. Endoscopically-assisted intradural dissection was then performed for downward migration of the cerebellum. This maneuver established a SCIT space and exposed the lower surface of the tentorium.

2.3 | Extreme-lateral eSCTT approach

A 3-cm-wide rectangular retrosigmoid craniotomy was performed by making a single vertical incision over the asterion; the transverse sinus and sigmoid sinus constituted the upper and lateral margins of the bone flap, respectively (Figure 2B). The dura was cut along the edge of the bone flap and deflected anterosuperiorly along the transverse and sigmoid sinuses; endoscopically-assisted intradural dissection was performed as described above.

2.4 | Establishing the grid coordinate system

A grid coordinate system based on pre-procedure navigation planning was applied to the tentorium (Figure 1B). The apex of the tentorium, located at the posterior edge of the tentorial incisura, was defined as the coordinate origin (0,0). The *X*-axis represented the left-to-right direction and the *X*-coordinates of points lateral to the coordinate origin were defined as positive. The *Y*-axis represented the front-to-back direction; the *Y*-coordinates of points anterior to the coordinate origin were defined as positive and those of points posterior to it were defined as negative. Colored pins were placed on the upper surface of the tentorium according to the planned coordinate points of the grid coordinate system; the pins were 1 cm apart from left to right on the *X*-axis and front to back on the *Y*-axis (Figures 1C and 3).

After this procedure was completed, the lower surface of the tentorium was inspected through the paramedian and extreme-lateral eSCTT approaches. Under endoscopic visualization, each colored pin was easily located by recognizing the position of the tip (Figure 2E). A digitizing probe was then used to acquire the desired data for the

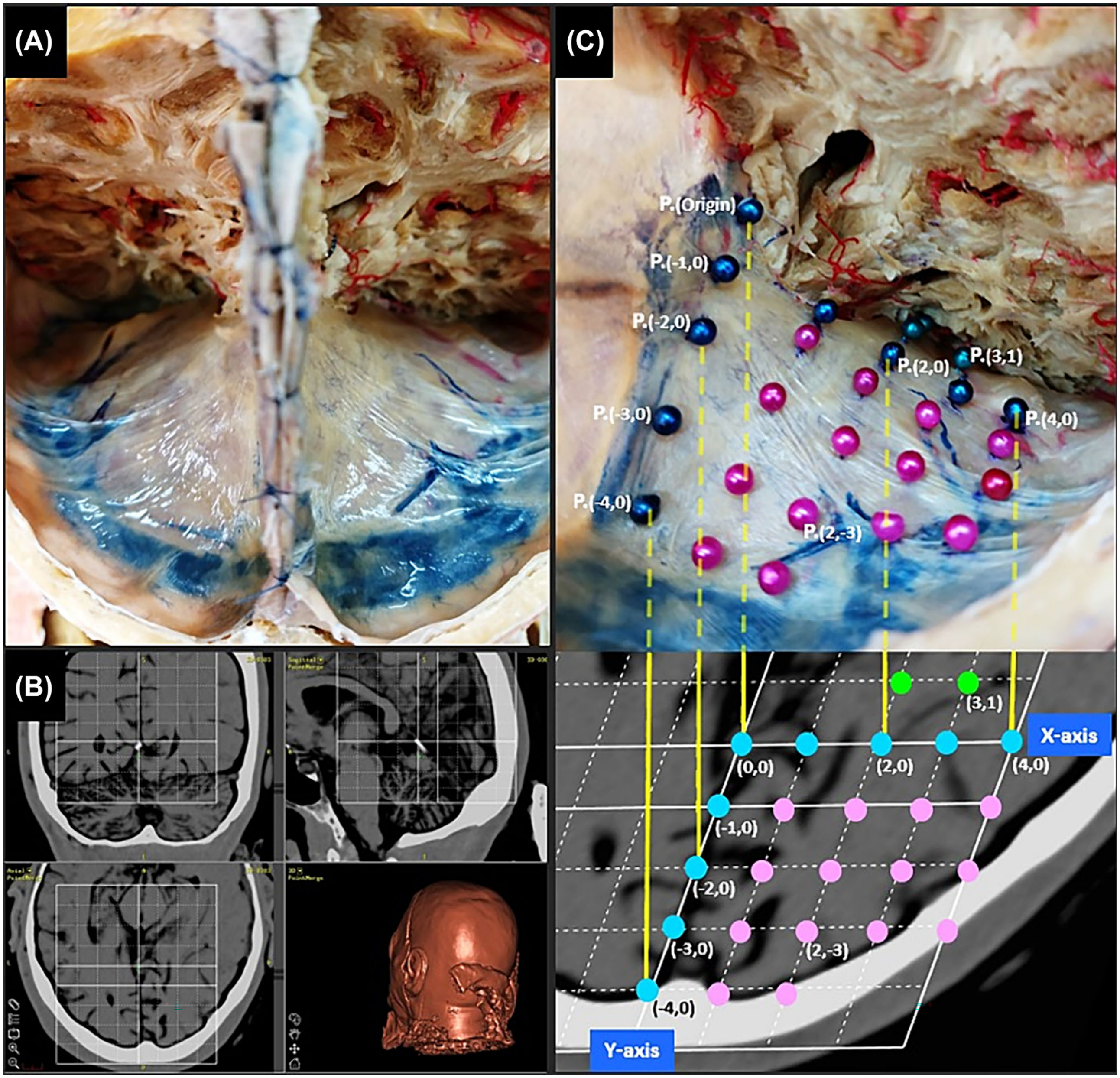

FIGURE 1 Establishment of the gird coordinate system. (A) Bilateral occipital lobes were resected to expose the tentorium. (B) The apex of the tentorium was defined as the coordinate origin, and a grid coordinate system was planned around the coordinate origin through pre-procedural navigation. (C) Colored pins were placed on the upper surface of the tentorium based on planned coordinate points of the grid coordinate system; the pins were placed 1 cm apart from left to right on the *X*-axis and front to back on the *Y*-axis.

selected points, including the angles of attack and depth of the surgical corridor (Figure 2F).

2.5 | Measurements

2.5.1 | Angle of attack

The angle of attack was defined as the maximum maneuverability of the surgical armamentarium on a specific target in the vertical and horizontal planes. For both eSCTT approaches, all colored pins were chosen as targets for measuring with a 20-cm digitizing probe. The angles in the vertical and horizontal planes were measured by fixing the distal end of the probe to a selected colored pin and moving the proximal end as far as possible in each plane.

2.5.2 | Depth of the surgical corridor

The distance measured from the bony flap to the selected colored pins was defined as the depth of the surgical corridor. The center of the exposed dura mater after bony drilling had been completed was defined as the representative position of the bone flap.

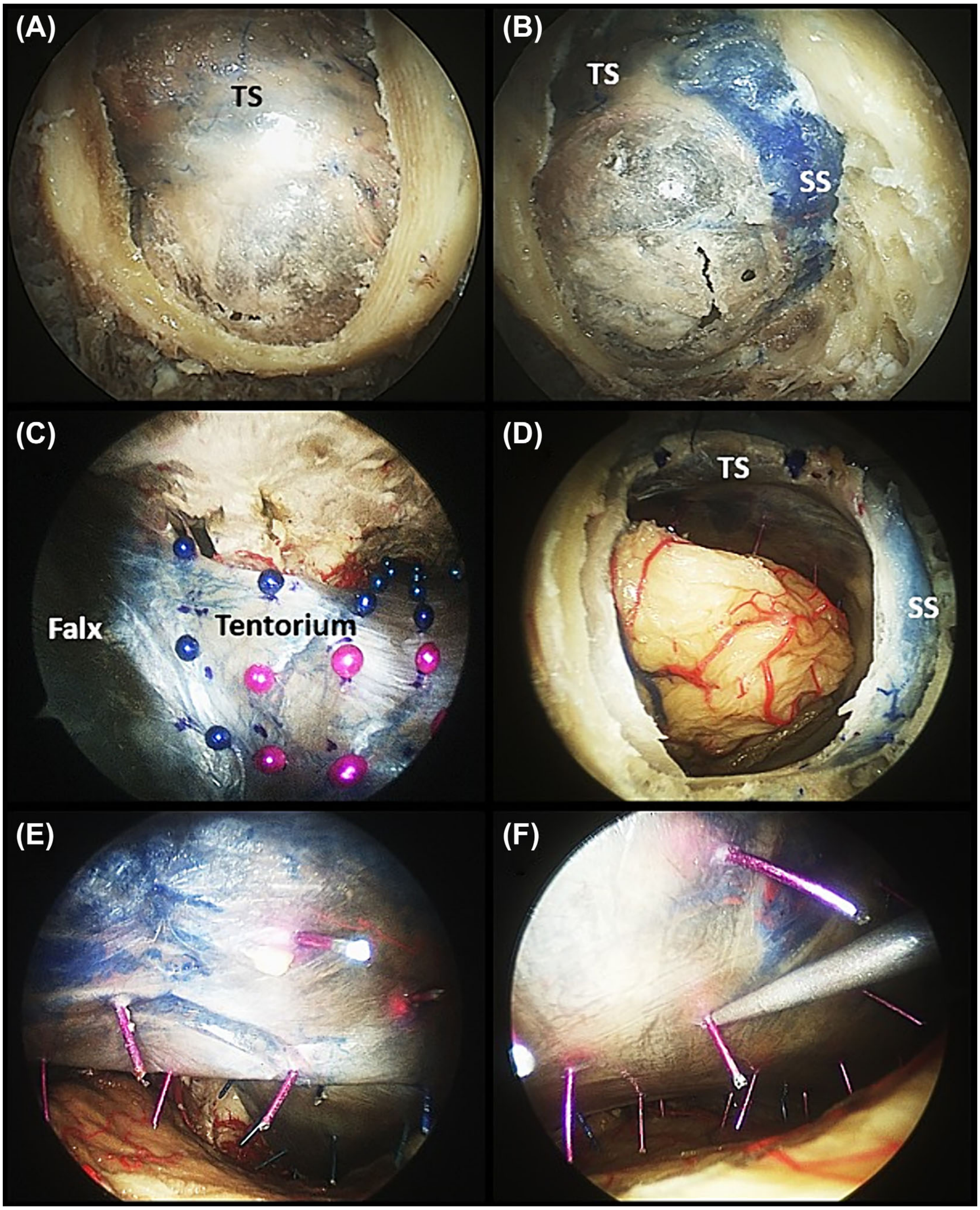

FIGURE 2 Description of how to take measurements through the endoscopically assisted supracerebellar transtentorial (eSCTT) approach. (A) Representative image of bony flap of paramedian eSCTT approach. (B) Representative image of bony flap of extreme-lateral eSCTT approach. (C) Endoscopic view of colored pins placed on the upper surface of the tentorium. (D) An extreme-lateral eSCTT approach was executed through retrosigmoid craniotomy. (E) Endoscopic view of the lower surface of the tentorium, showing the tip of each colored pin that represented the position of a planned coordinate point. (F) A digitizing probe was used to acquire the desired data, including the angle of attack and the depth of the surgical corridor, from the selected coordinate point. TS, transverse sinus; SS, sigmoid sinus.

2.5.3 | Statistical analysis

The average measurements were calculated using IBM IPSS Statistics 20 and presented as mean ± standard deviation. The angles of attack and depth of the surgical corridor were compared statistically between the paramedian and extreme-lateral eSCTT approaches using paired *t*-tests. Statistical significance was set at $p < 0.05$.

3 | RESULTS

3.1 | Establishment of the grid coordinate system

The size of the exposed tentorium differed between the cadaveric heads; therefore, only the coordinate points common to all cadaveric heads were considered in this study. Twenty-eight

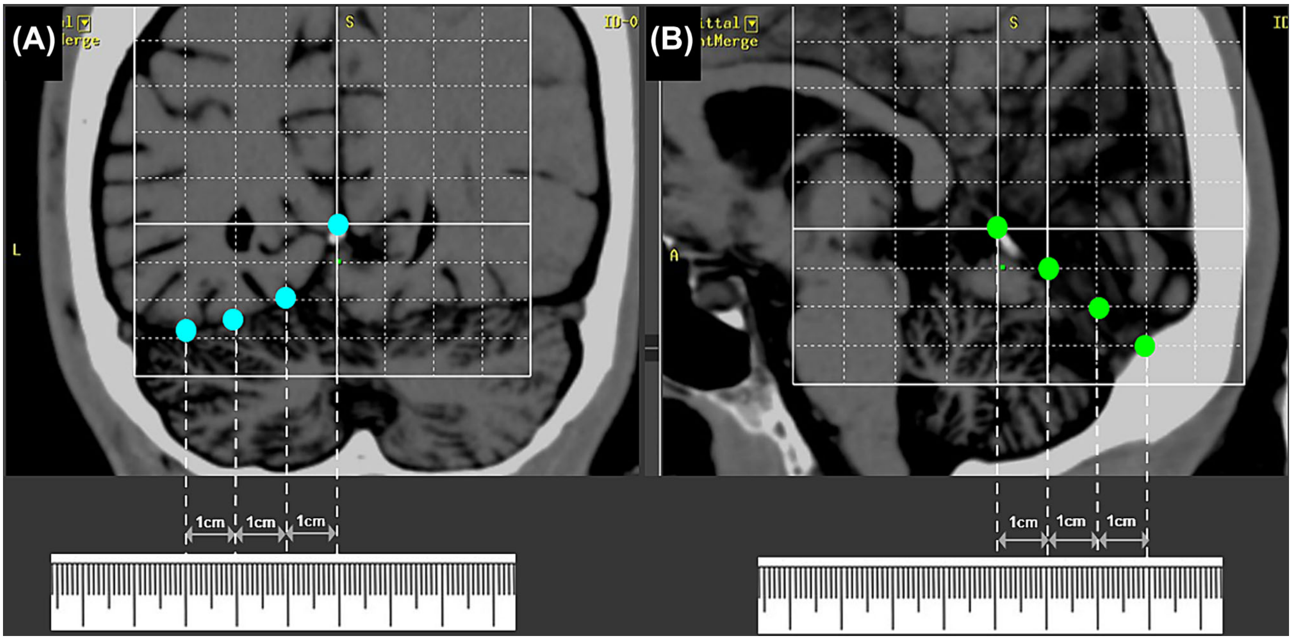

FIGURE 3 In the coronal (A) and sagittal (B) planes, the placement pattern of colored pins was evenly distributed when projected on to the horizontal plane.

coordinate points on each side of the tentorium were chosen for comparing the paramedian and extreme-lateral eSCTT approaches.

3.2 | Vertical angle of attack

Measurements of the vertical angle of attack are given in Table 1. At the coordinate points (2,2) and (3,1), the extreme-lateral eSCTT approach afforded a significantly greater vertical angle of attack than the paramedian eSCTT approach. At other coordinate points there was no significant difference between the two approaches (Figure 4A).

3.3 | Horizontal angle of attack

Measurements of the horizontal angle of attack are given in Table 2. At the coordinate points (2,0), (3,0), (4,0), (2,1), (3,1), (4,1), and (3,2), the extreme-lateral eSCTT approach had a significantly greater horizontal angle of attack than the paramedian variant. These seven points were aligned parallel to the horizontal line $Y = 1$.

At the coordinate points (0,0), (1,−3), and (2,−2), the paramedian eSCTT approach had a significantly greater horizontal angle of attack than the extreme-lateral variant (Figure 4B). These three points were symmetrically aligned along the vertical line $X = 1$.

3.4 | Depth of the surgical corridor

At the coordinate points (2,2), (3,1), (3,2), and (4,0), the extreme-lateral eSCTT approach had a significantly lower depth of surgical corridor than the paramedian variant (Table 3). These four points were symmetrically aligned along the vertical line $Y = 1$.

At the coordinate points (0,0), (0,−1), (0,−2), (0,−3), (1,0), (1,−1), (1,−2), (1,−3), and (2,−3), the paramedian eSCTT approach had a significantly lower depth of surgical corridor than the extreme-lateral variant (Figure 4C). These nine points were aligned parallel to the vertical line $X = 1$.

3.5 | Determining the conditions for selecting each eSCTT approach

On the basis of the foregoing findings, the relative anatomical relationship between each coordinate point and the bone flap affected the measurements of the horizontal angle of attack and the depth of the surgical corridor. For the paramedian eSCTT approach, statistically significant coordinate points were located near the vertical line $X = 1$. For the extreme-lateral eSCTT approach, statistically significant coordinate points were located near horizontal line $Y = 1$.

In summary, it appears that the paramedian SCTT approach was better when the long axis of the tumor projecting on to the tentorium was parallel to the Y-axis and was 1 cm outside the apex of the tentorium. In contrast, the extreme-lateral SCTT approach was better when the long axis of the tumor projecting on to the tentorium was parallel to the X-axis and 1 cm in front of the apex of the tentorium.

3.6 | Illustrative clinical cases

3.6.1 | Case 1

A 48-year-old woman presented with dizziness and unsteady gait for several weeks. Magnetic resonance imaging (MRI) of the brain showed a large homogeneously enhancing lesion consistent with a tentorial meningioma with supratentorial and infratentorial involvement. The

TABLE 1 Measurements of the vertical angle of attack in this study.

	Vertical angle of attack (°)			Vertical angle of attack (°)			Vertical angle of attack (°)			Vertical angle of attack (°)			Vertical angle of attack (°)	
CP	Ext-eSCTT	Para-eSCTT	CP	Ext-eSCTT	Para-eSCTT	CP	Ext-eSCTT	Para-eSCTT	CP	Ext-eSCTT	Para-eSCTT	CP	Ext-eSCTT	Para-eSCTT
	-	-		-	-	(2,3)	24.30 ± 0.46	15.67 ± 4.77	(3,3)	29.39 ± 0.90	17.96 ± 0.23		-	-
	-	-		-	-	(2,2)*	20.08 ± 6.81	14.52 ± 6.7	(3,2)	29.83 ± 8.69	24.03 ± 3.69		-	-
	-	-	(1,1)	20.71 ± 2.07	13.53 ± 1.33	(2,1)	21.09 ± 6.51	18.68 ± 7.56	(3,1)*	25.50 ± 6.04	18.04 ± 8.92		-	-
(0,0)	5.55 ± 2.98	8.77 ± 1.72	(1,0)	17.02 ± 5.78	18.17 ± 8.5	(2,0)	22.61 ± 6.45	18.51 ± 8.93	(3,0)	25.57 ± 3.88	23.66 ± 9.55	(4,0)	31.69 ± 6.91	23.18 ± 10.72
(0,−1)	9.32 ± 4.71	14.43 ± 2.94	(1,−1)	18.91 ± 5.29	18.49 ± 6.99	(2,−1)	20.53 ± 5.76	25.12 ± 10.39	(3,−1)	32.33 ± 13.58	29.64 ± 14.25	(4,−1)	33.45 ± 3.12	25.34 ± 11.00
(0,−2)	11.18 ± 5.53	20.59 ± 10.25	(1,−2)	18.68 ± 5.42	26.86 ± 8.98	(2,−2)	19.74 ± 6.73	29.03 ± 10.7	(3,−2)	26.63 ± 7.77	33.23 ± 18.37	(4,−2)	24.53 ± 4.60	24.73 ± 3.06
(0,−3)	7.86 ± 4.04	25.89 ± 10.69	(1,−3)	13.52 ± 2.25	31.21 ± 10.33	(2,−3)	19.34 ± 5.28	41.15 ± 18.16	(3,−3)	34.63 ± 2.56	24.11 ± 7.32		-	-
(0,−4)	13.77 ± 3.9	25.70 ± 3.38	(1,−4)	15.93 ± 0.74	26.92 ± 6.24	(2,−4)	25.00 ± 0.23	42.40 ± 4.59		-	-		-	-

Abbreviations: CP, coordinate point; Ext-eSCTT, extreme-lateral endoscopically assisted supracerebellar transtentorial approach; Para-eSCTT, paramedian endoscopically assisted supracerebellar transtentorial approach.

*Significant difference between Ext-eSCTT and Para-eSCTT.

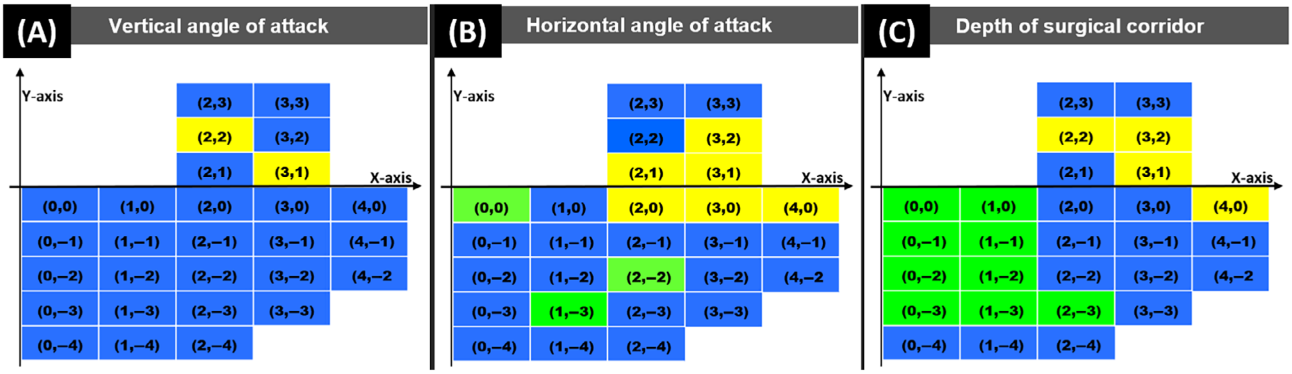

FIGURE 4 Comparative analysis of the paramedian and extreme-lateral eSCTT approaches from the perspective of the vertical angle of attack (A), horizontal angle of attack (B), and depth of the surgical corridor (C). Blue indicates no significant difference between the two approaches at that coordinate point. Green indicates that the paramedian SCTT approach is superior to the extreme-lateral SCTT approach, because a wider angle of attack or a shorter depth of surgical corridor is obtained at that coordinate point. Yellow indicates that the extreme-lateral SCTT approach is superior to the paramedian SCTT approach at that coordinate point.

extreme-lateral eSCTT approach in the semi-sitting position was used to resect the tumor and the patient made a full recovery with no neurological deficits. A definite histopathological report showed an atypical meningioma (World Health Organization grade II). She was followed up for 36 months with no evidence of recurrence (Figure 5). The intraoperative procedure is demonstrated in Video S1.

3.6.2 | Case 2

A 43-year-old woman presented with progressive left-sided weakness over several months. MRI of the brain revealed a large homogeneously enhancing lesion consistent with a meningioma in the right atrial region causing compression of the ipsilateral thalamus and the posterior limb of the internal capsule. The paramedian eSCTT approach in the semi-sitting position was used to remove the tumor. After the operation, the patient experienced temporary worsening of weakness in her left upper limb, but recovered completely within 3 months. This worsening could have resulted from inadvertent injury to the thalamus when the tumor was dissected away from its attachment (Figure 6J). The final histopathological report showed meningothelial meningioma (World Health Organization grade I). She was followed up for 24 months with no evidence of recurrence and no visual symptoms (Figure 6). The intraoperative procedure is demonstrated in Video S2.

3.6.3 | Case 3

A 58-year-old man presented to the emergency department complaining of a seizure. MRI of the brain showed an intra-axial tumor in the left medial temporo-occipital lobe, with heterogenous enhancement, peritumoral edema, and brain stem compression. The tumor was resected through the paramedian eSCTT approach in the semi-sitting position. The intraoperative frozen pathology report indicated high-grade glioma. The patient recovered well after surgery, and MRI immediately after surgery showed gross total resection of the tumor. The patient's histopathological report showed glioblastoma multiforme (World Health Organization grade IV). Unfortunately, the patient died 6 months later owing to tumor progression (Figure 7). The intraoperative procedure is demonstrated in Video S3.

4 | DISCUSSION

The medial temporo-occipital region, corresponding to the middle and posterior thirds of the medial temporal lobe, is difficult to approach owing to its deep location and surrounding white matter tracts (Campero et al., 2006). Several transcranial pathways, including pterional transsylvian, occipital interhemispheric, subtemporal, and transtemporal transventricular approaches, are reported to provide direct access to the target (Coca et al., 2022). According to the options for a surgical approach to the mediobasal temporal region proposed by Campero et al. (2006) and Türe et al. (2012), transcranial approaches to the medial temporo-occipital region have their own risks. The transsylvian approach cannot reach the posterior third of the medial temporal lobe. Subtemporal and transtemporal transventricular approaches have shorter surgical distances but entail risks of temporal lobe retraction, optic radiation injury, and language dysfunction. The occipital interhemispheric approach provides direct access to the posterior third of the medial temporal, but is only suitable for limited lesions. Larger tumors can require significant occipital lobe retraction, with accompanying visual field defects. "Long transparenchymal dissection" does not refer to the length of the surgical corridor, but rather to the excessive destruction of normal brain tissue during dissection.

The SCTT approach to the medial temporo-occipital region is renowned for its limited destruction of normal brain parenchyma; its clinical application is widespread because the risk of associated morbidity is low (de Oliveira et al., 2010; Marcus et al., 2013; Türe

TABLE 2 Measurements of the horizontal angle of attack in this study.

CP	Horizontal angle of attack (°)		CP	Horizontal angle of attack (°)		CP	Horizontal angle of attack (°)		CP	Horizontal angle of attack (°)		CP	Horizontal angle of attack (°)	
	Ext-eSCTT	Para-eSCTT		Ext-eSCTT	Para-eSCTT		Ext-eSCTT	Para-eSCTT		Ext-eSCTT	Para-eSCTT		Ext-eSCTT	Para-eSCTT
	-	-		-	-	(2,3)	29.4 ± 9.42	23.07 ± 8.1	(3,3)	28.90 ± 12.90	22.91 ± 3.62		-	-
	-	-		-	-	(2,2)	25.89 ± 13.57	19.59 ± 8.65	(3,2)*	37.23 ± 11.72	22.95 ± 5.91		-	-
	-	-	(1,1)	26.83 ± 0.56	20.85 ± 5.38	(2,1)*	33.88 ± 10.29	24.66 ± 5.65	(3,1)*	33.87 ± 8.49	24.43 ± 9.81		-	-
(0,0)*	11.15 ± 9.27	17.07 ± 8.47	(1,0)	30.18 ± 8.38	30.31 ± 9.3	(2,0)*	35.30 ± 8.19	30.19 ± 7.02	(3,0)*	42.34 ± 13.51	30.84 ± 13.13	(4,0)*	47.78 ± 22.91	25.98 ± 12.76
(0,−1)	20.38 ± 6.42	19.13 ± 7.76	(1,−1)	28.83 ± 5.96	28.02 ± 8.65	(2,−1)	35.46 ± 12.69	41.74 ± 13.09	(3,−1)	45.05 ± 6.51	37.81 ± 13.44	(4,−1)	40.7 ± 12.44	22.18 ± 4.85
(0,−2)	21.74 ± 8.13	24.51 ± 12.2	(1,−2)	28.56 ± 8.23	39.04 ± 7.42	(2,−2)*	32.42 ± 8.34	49.86 ± 10.07	(3,−2)	35.23 ± 9.52	46.86 ± 24.57	(4,−2)	50.52 ± 9.98	21.85 ± 7.12
(0,−3)	23.09 ± 7.86	28.93 ± 7.55	(1,−3)*	21.50 ± 3.92	40.3 ± 7.05	(2,−3)	27.68 ± 6.31	56.69 ± 14.11	(3,−3)	41.03 ± 5.62	45.22 ± 4.05		-	-
(0,−4)	11.57 ± 1.83	25.64 ± 1.33	(1,−4)	20.66 ± 1.56	49.51 ± 3.58	(2,−4)	17.01 ± 0.8	63.44 ± 11.53		-	-		-	-

Abbreviations: CP, coordinate point; Ext-eSCTT, extreme-lateral endoscopically assisted supracerebellar transtentorial approach; Para-eSCTT, paramedian endoscopically assisted supracerebellar transtentorial approach.

*Significant difference between Ext-eSCTT and Para-eSCTT.

TABLE 3 Measurements of the depth of the surgical corridor in this study.

CP	Surgical corridor depth (mm)		CP	Surgical corridor depth (mm)		CP	Surgical corridor depth (mm)		CP	Surgical corridor depth (mm)		CP	Surgical corridor depth (mm)	
	Ext-eSCTT	Para-eSCTT		Ext-eSCTT	Para-eSCTT		Ext-eSCTT	Para-eSCTT		Ext-eSCTT	Para-eSCTT		Ext-eSCTT	Para-eSCTT
	-	-		-	-	(2,3)	43.11 ± 5.48	57.88 ± 2.47	(3,3)	34.80 ± 5.67	59.48 ± 3.30		-	-
	-	-		-	-	(2,2)*	45.34 ± 8.18	55.59 ± 8.12	(3,2)*	32.62 ± 5.47	50.12 ± 6.49		-	-
	-	-	(1,1)	47.66 ± 0.20	47.46 ± 0.59	(2,1)	40.97 ± 8.01	49.12 ± 7.9	(3,1)*	33.34 ± 6.59	48.43 ± 10.34		-	-
(0,0)*	68.32 ± 4.16	60.27 ± 6.05	(1,0)*	48.57 ± 6.19	43.01 ± 5.32	(2,0)	38.13 ± 4.60	42.53 ± 8.09	(3,0)	28.88 ± 6.36	40.82 ± 11.13	(4,0)*	23.18 ± 6.35	42.40 ± 12.17
(0,−1)*	60.40 ± 4.40	47.27 ± 6.22	(1,−1)*	46.14 ± 5.51	38.49 ± 6.52	(2,−1)	36.18 ± 4.53	33.10 ± 8.76	(3,−1)	28.86 ± 3.34	33.43 ± 10.71	(4,−1)	24.81 ± 1.29	40.29 ± 7.55
(0,−2)*	53.93 ± 6.05	35.56 ± 7.46	(1,−2)*	43.53 ± 3.87	30.40 ± 6.50	(2,−2)*	34.84 ± 3.31	26.87 ± 7.40	(3,−2)	27.77 ± 2.04	30.84 ± 8.99	(4,−2)	20.41 ± 1.70	38.45 ± 0.16
(0,−3)*	53.53 ± 5.63	32.26 ± 4.61	(1,−3)*	44.15 ± 4.12	27.04 ± 3.01	(2,−3)*	37.82 ± 4.65	23.60 ± 2.57	(3,−3)	26.44 ± 0.48	28.77 ± 0.70		-	-
(0,−4)	54.92 ± 5.39	26.90 ± 1.19	(1,−4)	45.81 ± 3.69	24.04 ± 1.46	(2,−4)	38.31 ± 3.93	20.24 ± 1.74		-	-		-	-

Abbreviations: CP, coordinate point; Ext-eSCTT: extreme-lateral endoscopically assisted supracerebellar transtentorial approach; Para-eSCTT: paramedian endoscopically assisted supracerebellar transtentorial approach.

*Significant difference between Ext-eSCTT and Para-eSCTT.

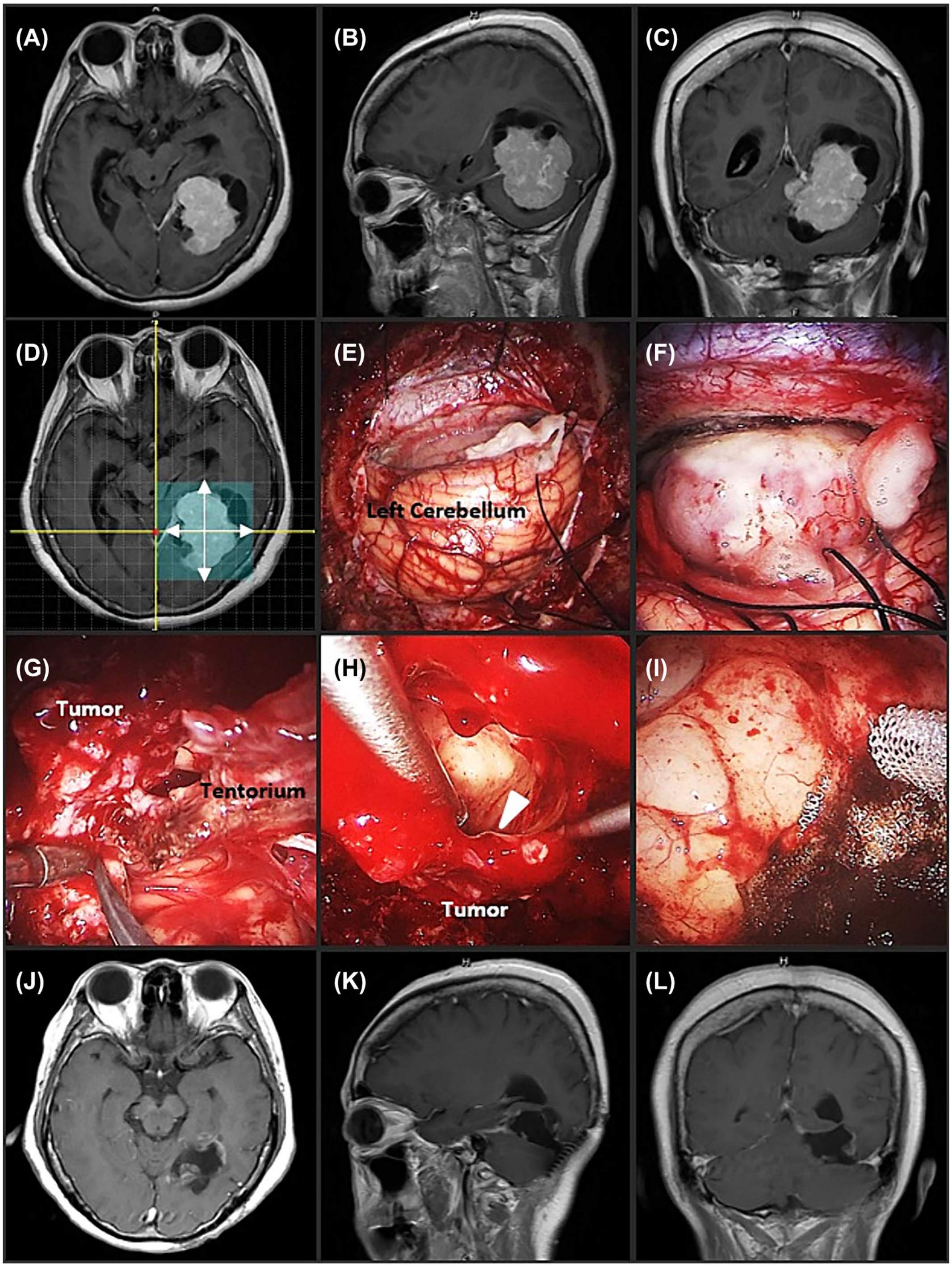

FIGURE 5 Illustrative case number 1. Preoperative axial (A), sagittal (B), and coronal (C) contrast-enhanced T1-weighted magnetic resonance (MR) images obtained from a 48-year-old woman with a left-sided tentorial meningioma. The tumor projecting into the tentorium has a round configuration. Two axes of the tumor are identified; the vertical axis is parallel to the *Y*-axis and 4 cm outside the apex of the tentorium, and the horizontal axis is located on the *X*-axis (D). Because the horizontal axis of the tumor was close to the selection criteria of the extreme-lateral supracerebellar transtentorial (SCTT) approach, the left-sided extreme-lateral SCTT approach was chosen (E). We first removed the infratentorial compartment of the tumor (F), followed by the transtentorial approach to reach the supratentorial compartment (G). Using a 30-degree endoscope, it was easy to see the brain–tumor interface (H, the position of the arrowhead is the upper edge of the tumor) and achieve complete tumor resection (I). Postoperative axial (J), sagittal (K), and sagittal (L) contrast-enhanced T1-weighted MR images showing gross total resection of the tumor.

et al., 2012; Weil et al., 2015). The main disadvantages of the SCTT approach to treating supratentorial pathology are reduced illumination and visualization of the deeply seated surgical field, and a narrow surgical corridor. When a seated position is assumed, the cerebellum spontaneously moves downward under the influence of gravity, forming a wide SCIT space, which increases instrument maneuverability. In

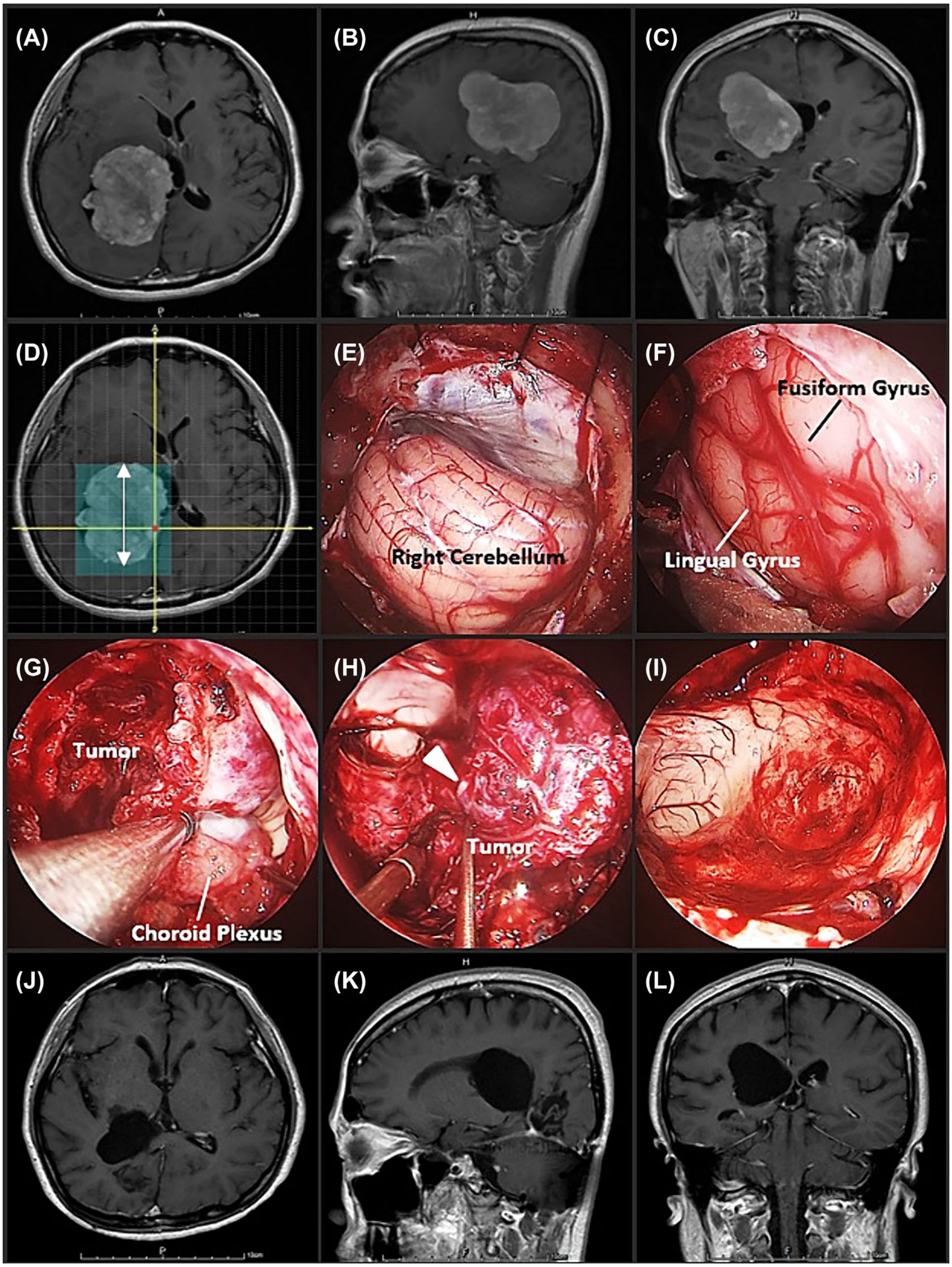

FIGURE 6 Illustrative case number 2. Preoperative axial (A), sagittal (B), and coronal (C) contrast-enhanced T1-weighted magnetic resonance (MR) images obtained from a 43-year-old woman with a right-sided atrial meningioma. The long axis of the tumor was parallel to the *Y*-axis and 2 cm outside the apex of the tentorium (D). Because it was close to the selection criteria of the paramedian supracerebellar transtentorial (SCTT) approach, the right-sided paramedian SCTT approach was chosen (E). After the tentorium cut, the transcollateral sulcus approach (F) was adopted to gain entry into the ventricular atrium. Following surgical debulking of the tumor, the lateral posterior choroidal artery attached to the choroid plexus was coagulated and incised to control tumor bleeding. Using a 30-degree endoscope, it was easy to see the brain–tumor interface (H, the position of the arrowhead is the upper edge of the tumor) and achieve complete tumor resection (I). Postoperative axial (J), sagittal (K), and sagittal (L) contrast-enhanced T1-weighted MR images showing gross total resection of the tumor.

the present study, our surgical target was medial temporo-occipital region, and release of cerebrospinal fluid from the lateral cerebellomesencephalic cistern was sufficient to establish the SCIT working space. If necessary, the bridging veins over the tentorium can be sacrificed to relax the cerebellum further. However, the sharp tilt of the tentorium can impede the surgical field and cause ergonomic discomfort.

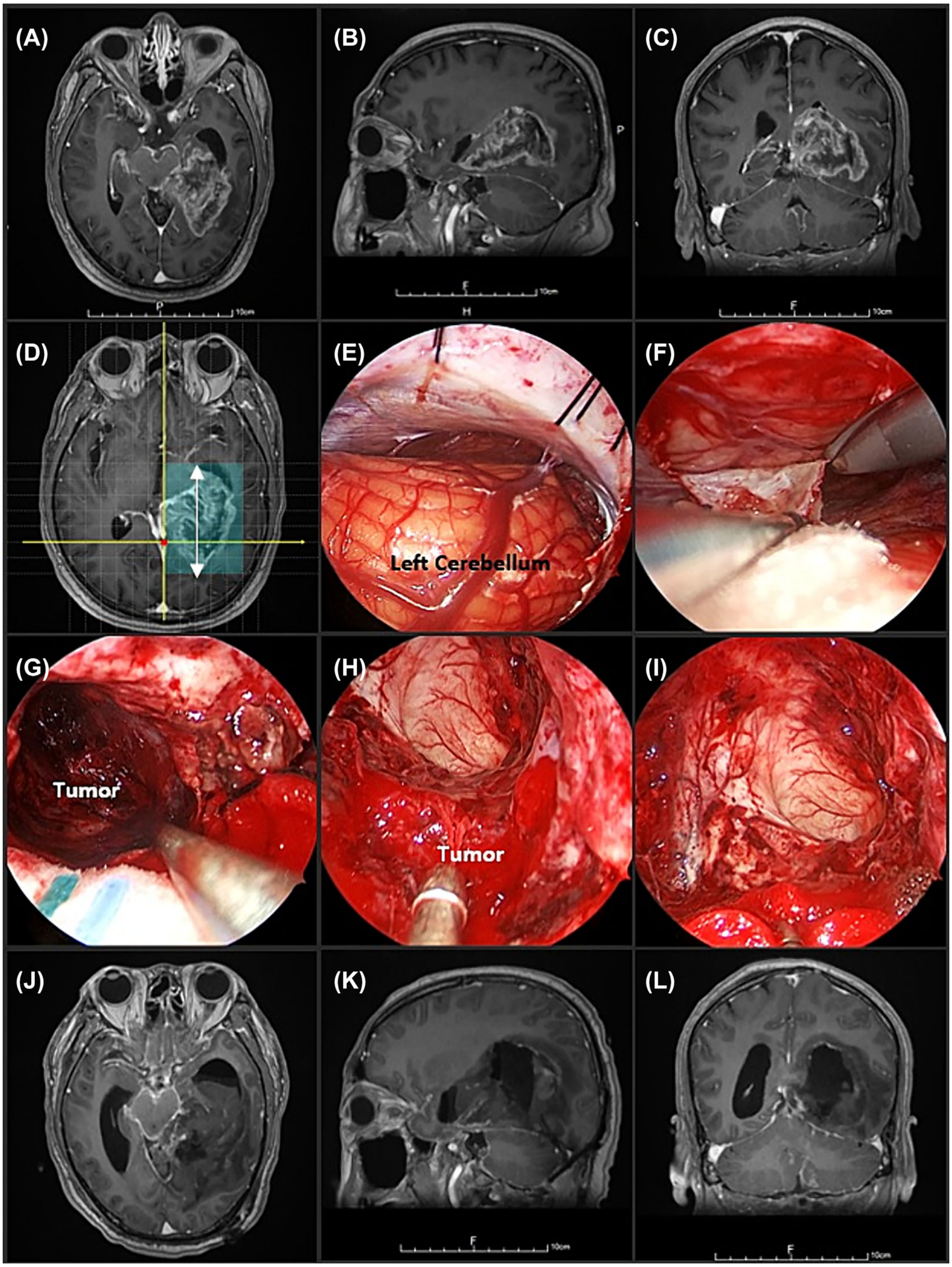

FIGURE 7 Illustrative case number 3. Preoperative axial (A), sagittal (B), and coronal (C) contrast-enhanced T1-weighted MR images obtained from a 58-year-old man with a glioblastoma multiforme in the left-sided medial temporo-occipital region. The long axis of the tumor was parallel to the *Y*-axis and 2 cm outside the apex of the tentorium (D). Because it was close to the selection criteria of the paramedian supracerebellar transtentorial (SCTT) approach, the left paramedian SCTT approach was chosen (E). After incising the tentorium (F), the tumor was identified by sacrificing a small amount of brain parenchyma at the base of the occipital lobe (G). The endoscope provided clear illumination and good magnification over the deep-seated surgical field (H) and helped tumor removal under direct visualization (I). Immediate postoperative axial (J), sagittal (K), and sagittal (L) contrast-enhanced T1-weighted magnetic resonance images showing near-total resection of the tumor.

Although modifications of the tentorium cut can improve visualization of the supratentorial space, they still do not provide a clear circumferential view around the supratentorial lesion, especially if the tumor edge is located far above the tentorium (Berker et al., 2023; de Oliveira et al., 2012).

The endoscope is used to overcome the limitations of microscopy because of its better illumination, higher magnification, and wider operative view. During the eSCTT approach, angled endoscopes are valuable for identifying the boundary between a tumor in the medial temporo-occipital region and normal brain tissues, especially when the upper edge of the tumor is some distance away from the tentorium. This panoramic visualization prevents inadvertent injury to surrounding structures owing to a limited surgical field of view. On the other hand, the precise coordination between instrument handling and visualization with angled endoscopes involves a steep learning curve. Bleeding control is also important; early recognition and careful hemostasis are necessary for maintaining clear visualization with angled endoscopes when the eSCTT approach is performed. In the event of massive bleeding, an effective treatment modality is temporary compression with cotton to make the bleeding point easier to locate with an angled endoscope.

Previous studies have reported promising results with the eSCTT approach to lesions in the medial temporo-occipital region (Coca et al., 2022; Marcus et al., 2013; Villanueva et al., 2015). For relatively small tumors, preoperative planning often favored a shorter, more direct surgical path based on a navigation system to minimize injury to normal brain tissue. For large tumors, the anatomical relationships between tumor location, the slope of the tentorium, and the design of the suboccipital bone flap need to be analyzed during preoperative planning. The benefits of establishing a more lateral suboccipital craniotomy in the SCIT approach to the pineal region and posterolateral incisural space include relative deficiency of a tentorial bridging vein, more direct lateral mesencephalic sulcus visualization, and improved instrument maneuverability (Cavalcanti et al., 2019; Matsuo et al., 2017; Zaidi et al., 2015). The effects of different suboccipital craniotomies on managing supratentorial lesions during the SCTT approach have not been discussed, and no study to date has analyzed this important issue quantitatively.

In this study, we used a grid coordinate system established on the tentorium to model the anatomy between the pathology in the medial temporo-occipital region and the slope of the tentorium in the sitting position. The sitting position, first introduced by de Martel, was criticized because of its risk of venous air embolism (de Martel, 1931). A modified variant, the so-called semi-sitting position, was proposed and achieved a low risk of venous air embolism in standardized clinical use, and it was proven to be hemodynamically safe (Ammirati et al., 2013; Jadik et al., 2009; Luostarinen et al., 2017). The force of gravity helps to establish the dissection plane between the upper portion of the tumor and surrounding brain parenchyma after the lower portion of the tumor is removed. This maneuver causes the upper portion of the tumor to fall downwards toward the tentorium. In our grid coordinate system, colored pins placed on the tentorium represented the coordinate points for quantification. If the colored pins were evenly and sequentially placed on the tentorium, different cadaveric heads could not be compared quantitatively because the slopes of the tentorium vary. Under the conditions we set up, successive coordinate points in this system were set to be 1 cm apart from left to right and front to back on the horizontal projection plane. This setting facilitated objective comparison of each cadaveric head with different tentorial slopes. Since a single large lesion can occupy multiple coordinate points on the grid coordinate system, we analyzed coordinate points and their corresponding measurements provided by different suboccipital craniotomies to represent the different SCTT approaches to reach the medial temporo-occipital region.

During measurements, the vertical movement of the digitizing probe for each coordinate point was primarily constrained by the limited space between the tentorium and the upper surface of the cerebellum. This showed that the measurements at each coordinate point were not significantly different because of the relative position of each coordinate point and the bone flap. It also indicated that the difference between the two eSCTT approaches was not significant. On the other hand, the width of the bone flap constituted the primary determinant of the horizontal movement of the digitizing probe. We observed that the relative anatomical relationship between each coordinate point and the bone flap greatly influenced the measurements of the horizontal angle of attack and the depth of the surgical corridor.

By analyzing the distribution of coordinate points that were statistically significant in terms of the horizontal angle of attack and the depth of the surgical corridor, we found that the projection of the long axis of the tumor facilitated the selection of the appropriate approach. This long axis was projected on to the tentorium, and its corresponding coordinate points were used to match the suitable eSCTT approach. On the one hand, the paramedian SCTT approach was considered first if the long axis of the tumor projecting on to the tentorium was parallel to the *Y*-axis and 1 cm outside the apex of the tentorium. On the other, the extreme-lateral SCTT approach was more suitable if the long axis of the tumor projecting on to the tentorium was parallel to the *X*-axis and 1 cm in front of the apex of the tentorium. We applied this selection strategy to three cases of large tumors in the medial temporo-occipital region and achieved satisfactory results.

This study is the first quantitative analysis of the application of different eSCTT approaches to reach the medial temporo-occipital region. Despite the encouraging initial outcomes for our patients, the study has several limitations. It was a postmortem study of formalin-fixed brain tissue with only three cadaveric heads, and the analyses presented here cannot fully represent in vivo results. The grid coordinate system used to interpret the results was based on the assumption that the upper portion of the tumor will collapse under gravity on to the level of the tentorium after the lower portion has been removed. This treatment strategy must be used in situations where there is a clear dissection plane between the tumor and normal brain parenchyma. Moreover, this grid coordinate system is not suitable for patients with lesions tightly adherent to supratentorial structures or for patients scheduled to undergo surgery in other positions. Moreover, our study took no account of the distribution of the tentorial bridging veins on the hemispheres, which could complicate intraoperative dissection. More clinical cases are needed to verify the reliability of the present results. Clinical decisions should be judged on the basis of the specific parameters of each patient.

5 | CONCLUSION

In clinical practice, applying the eSCTT approach to deal with tumors in the medial temporo-occipital region can avoid unnecessary brain injury caused by the transcortical approach. This is important for patients at risk of language and visual impairments, particularly when tumors are located in the dominant hemisphere. Projection of the long axis of the tumor on to the tentorium can help clinicians to design customized eSCTT approach preoperatively to treat larger ones safely and effectively.

FUNDING INFORMATION

The work was supported by the Tri-Service General Hospital of Taiwan's Medical Research Project (TSGH-D-111088 and TSGH-D-112095).

DATA AVAILABILITY STATEMENT

The datasets generated during and/or analyzed during the current study are available from the corresponding author on reasonable request.

INFORMED CONSENT

Informed consent was obtained from all individual participants included in the study.

ORCID

Bon-Jour Lin https://orcid.org/0000-0003-4862-6697

REFERENCES

Ammirati, M., Lamki, T. T., Shaw, A. B., Forde, B., Nakano, I., & Mani, M. (2013). A streamlined protocol for the use of the semi-sitting position in neurosurgery: A report on 48 consecutive procedures. *Journal of Clinical Neuroscience*, *20*, 32–34.

Berker, B. B., Doğruel, Y., Güngör, A., Karataş Okumuş, S. Y., Coşkun, M. E., Türe, H., & Türe, U. (2023). Preserving the cerebellar hemispheric tentorial bridging veins through a novel tentorial cut technique for supracerebellar approaches. *Journal of Neurosurgery*, *140*, 260–270.

Campero, A., Tróccoli, G., Martins, C., Fernandez-Miranda, J. C., Yasuda, A., & Rhoton, A. L., Jr. (2006). Microsurgical approaches to the medial temporal region: An anatomical study. *Neurosurgery*, *59*(4 Suppl 2), ONS279–ONS307.

Cavalcanti, D. D., Morais, B. A., Figueiredo, E. G., Spetzler, R. F., & Preul, M. C. (2019). Surgical approaches for the lateral mesencephalic sulcus. *Journal of Neurosurgery*, *132*, 1653–1658.

Coca, A., Ganau, M., Todeschi, J., Zaed, I., Dannhoff, G., Mallereau, C. H., Romano, A., Cebula, H., Santin, M. D. N., Proust, F., Bruno, C., Nannavecchia, B., Savarese, L., Pop, R., Baloglu, S., & Chibbaro, S. (2022). Endoscopic-enhanced supra-cerebellar trans-tentorial (SCTT) approach to temporo-mesial region: a multicenter study. *Neurosurgical Review*, *45*, 3749–3758.

de Martel, T. (1931). Surgical treatment of cerebral tumours. Technical considerations. *Surgery, gynecology & obstetrics*, *52*, 381–385.

de Oliveira, J. G., Lekovic, G. P., Safavi-Abbasi, S., Reis, C. V., Hanel, R. A., Porter, R. W., Preul, M. C., & Spetzler, R. F. (2010). Supracerebellar infratentorial approach to cavernous malformations of the brainstem: Surgical variants and clinical experience with 45 patients. *Neurosurgery*, *66*, 389–399.

de Oliveira, J. G., Párraga, R. G., Chaddad-Neto, F., Ribas, G. C., & de Oliveira, E. P. (2012). Supracerebellar transtentorial approach-resection of the tentorium instead of an opening-to provide broad exposure of the mediobasal temporal lobe: Anatomical aspects and surgical applications: Clinical article. *Journal of Neurosurgery*, *116*, 764–772.

Jadik, S., Wissing, H., Friedrich, K., Beck, J., Seifert, V., & Raabe, A. (2009). A standardized protocol for the prevention of clinically relevant venous air embolism during neurosurgical interventions in the semisitting position. *Neurosurgery*, *64*, 533–538.

Luostarinen, T., Lindroos, A. C., Niiya, T., Silvasti-Lundell, M., Schramko, A., Hernesniemi, J., Randell, T., & Niemi, T. (2017). Prone versus sitting position in neurosurgery-differences in patients' hemodynamic management. *World Neurosurgery*, *97*, 261–266.

Marcus, H. J., Sarkar, H., Mindermann, T., & Reisch, R. (2013). Keyhole supracerebellar transtentorial transcollateral sulcus approach to the lateral ventricle. *Neurosurgery*, *73*(2 Suppl Operative), onsE295–onsE301.

Matsuo, S., Baydin, S., Güngör, A., Miki, K., Komune, N., Kurogi, R., Iihara, K., & Rhoton, A. L., Jr. (2017). Midline and off-midline infratentorial supracerebellar approaches to the pineal gland. *Journal of Neurosurgery*, *126*, 1984–1994.

Türe, U., Harput, M. V., Kaya, A. H., Baimedi, P., Firat, Z., Türe, H., & Bingöl, C. A. (2012). The paramedian supracerebellar-transtentorial approach to the entire length of the mediobasal temporal region: An anatomical and clinical study Laboratory investigation. *Journal of Neurosurgery*, *116*, 773–791.

Villanueva, P., Louis, R. G., Cutler, A. R., Wei, H., Sale, D., Duong, H. T., Barkhoudarian, G., & Kelly, D. F. (2015). Endoscopic and gravity-assisted resection of medial temporo-occipital lesions through a supracerebellar transtentorial approach: Technical notes with case illustrations. *Operative neurosurgery (Hagerstown)*, *11*, 475–483.

Voigt, K., & Yasargil, M. G. (1976). Cerebral cavernous haemangiomas or cavernomas.Incidence, pathology, localization, diagnosis, clinical features and treatment. Review of the literature and report of an unusual case. *Neurochirurgia (Stuttg)*, *19*, 59–68.

Weil, A. G., Middleton, A. L., Niazi, T. N., Ragheb, J., & Bhatia, S. (2015). The supracerebellar-transtentorial approach to posteromedial temporal lesions in children with refractory epilepsy. *Journal of Neurosurgery. Pediatrics*, *15*, 45–54.

Zaidi, H. A., Elhadi, A. M., Lei, T., Preul, M. C., Little, A. S., & Nakaji, P. (2015). Minimally invasive endoscopic supracerebellar-infratentorial surgery of the pineal region: Anatomical comparison of four variant approaches. *World Neurosurgery*, *84*, 257–266.

SUPPORTING INFORMATION

Additional supporting information can be found online in the Supporting Information section at the end of this article.

How to cite this article: Lin, B.-J., Ju, D.-T., Lin, C., Hueng, D.-Y., Chen, Y.-H., Ma, H.-I., & Liu, M.-Y. (2024). Optimizing the selection of the endoscopically assisted supracerebellar transtentorial approach to the medial temporo-occipital region: Clinical application of one novel grid coordinate system. *Clinical Anatomy*, 1–14. https://doi.org/10.1002/ca.24208